

Published in final edited form as:

Free Radic Biol Med. 2013 December ; 65: 1047–1059. doi:10.1016/j.freeradbiomed.2013.08.170.

Inhibitors of ROS production by the ubiquinone-binding site of mitochondrial complex I identified by chemical screening

Adam L. Orr¹, Deepthi Ashok, Melissa R. Sarantos, Tong Shi², Robert E. Hughes, and Martin D. Brand

Buck Institute for Research on Aging, Novato, California 94945, USA

Abstract

Mitochondrial production of reactive oxygen species is often considered an unavoidable consequence of aerobic metabolism and currently cannot be manipulated without perturbing oxidative phosphorylation. Antioxidants are widely used to suppress effects of reactive oxygen species after formation, but they can never fully prevent immediate effects at the sites of production. To identify site-selective inhibitors of mitochondrial superoxide/H₂O₂ production that do not interfere with mitochondrial energy metabolism, we developed a robust small-molecule screen and secondary profiling strategy. We describe the discovery and characterization of a compound (N-cyclohexyl-4-(4-nitrophenoxy)benzenesulfonamide; CN-POBS) that selectively inhibits superoxide/H₂O₂ production from the ubiquinone-binding site of complex I (site I_Q) with no effects on superoxide/H₂O₂ production from other sites or on oxidative phosphorylation. Structure/activity studies identified a core structure that is important for potency and selectivity for site I_Q. By employing CN-POBS in mitochondria respiring on NADH-generating substrates, we show that site I_Q does not produce significant amounts of superoxide/H₂O₂ during forward electron transport on glutamate plus malate. Our screening platform promises to facilitate further discovery of direct modulators of mitochondrially-derived oxidative damage and advance our ability to understand and manipulate mitochondrial reactive oxygen species production in both normal and pathological conditions.

Keywords

superoxide; hydrogen peroxide; antioxidant; glycerol 3-phosphate dehydrogenase; NADH:Q oxidoreductase; complex II; complex III; energy metabolism; respiratory complexes

© 2013 Elsevier Inc. All rights reserved.

¹Corresponding author. aorr@buckinstitute.org (Adam L. Orr).

²Present address: Evotec, 385 Oyster Point Blvd, Suite 1, South San Francisco, CA 94080, USA

Publisher's Disclaimer: This is a PDF file of an unedited manuscript that has been accepted for publication. As a service to our customers we are providing this early version of the manuscript. The manuscript will undergo copyediting, typesetting, and review of the resulting proof before it is published in its final citable form. Please note that during the production process errors may be discovered which could affect the content, and all legal disclaimers that apply to the journal pertain.

Author contributions

Adam Orr designed, performed, and analyzed all experiments. Deepthi Ashok assisted with screening, mitochondrial respiration, and TPMP measurements. Melissa Sarantos and Tong Shi assisted with screening. Robert Hughes provided the chemical library and advised in the design, execution, and analysis of the screen. Martin Brand conceived and oversaw the project. Adam Orr and Martin Brand wrote the paper.

INTRODUCTION

Mitochondrial production of reactive oxygen species (ROS) is central to the free radical theory of aging [1] and implicated in the pathogenesis of virtually all age-associated diseases including cardiovascular disease, neurodegeneration, cancer and diabetes [2–6]. Most research on the roles of ROS in aging and disease has focused on two areas: defining the mechanisms and sites of ROS production under normal and pathogenic conditions, and developing broad-acting antioxidants to decrease damage caused by ROS. Considerable progress has been made in defining sites of production and it is generally accepted that at least ten distinct sites exist within mitochondria [7]. Although mitochondrial production of superoxide and/or H_2O_2 has been implicated in a wide range of pathological events, the current inability to dissociate it from energy metabolism has made attribution to any site equivocal at best. Further, the contribution of each (or any) site under normal circumstances remains completely unknown.

Complex I and complex III have high capacities for production of superoxide/ H_2O_2 and are commonly stated to be the sites most relevant to disease [8], although there is scant evidence for this view. In complex I, there is evidence for the existence of two sites of superoxide/ H_2O_2 production, the flavin binding site (site I_F) and the ubiquinone-binding site (site I_Q) [9]. Site I_Q generates superoxide/ H_2O_2 at high rates during reverse electron flow from a reduced ubiquinone pool and is dependent upon a high protonmotive force across the mitochondrial inner membrane. In contrast, site I_F is prominent during forward electron flow from a reduced NADH pool in the mitochondrial matrix and has a much lower maximum rate of production than site I_Q in intact mitochondria. Blockade of site I_Q by rotenone potently inhibits superoxide/ H_2O_2 production from site I_Q by preventing oxidation of ubiquinone and reverse electron transport into the site. In contrast, rotenone potentiates superoxide production from site I_F by increasing its reduction state [9]. Inhibition of complex I activity by rotenone or the neurotoxin MPP⁺ has been linked to parkinsonism in both rodents and humans suggesting a link between dysfunctional complex I, ROS production, and neurodegeneration [10, 11]. In contrast, comparative analyses show an inverse relationship between maximal superoxide/ H_2O_2 production from site I_Q , but not site I_F , and maximum life span across diverse vertebrate species [12, 13]. Therefore, selective modulators of superoxide/ H_2O_2 production from site I_Q or site I_F would offer unique opportunities to probe the putative role of mitochondrial ROS production in normal and pathological processes.

The outer ubiquinone-binding site of complex III (site III_{Q_o}) has the highest absolute capacity for superoxide production of all sites identified [14], partly because of the relative abundance of complex III. Although these high rates occur in the presence of the complex III inhibitor antimycin A, this site is active even in mitochondria respiring on different substrates in the absence of inhibitors [15, 16]. Site III_{Q_o} and mitochondrial glycerol 3-phosphate dehydrogenase (mGPDH) are distinguished from the other sites by their production of superoxide to both the matrix and cytosolic sides of the mitochondrial inner membrane [17, 18]. This fact, combined with the reported high rates of production from site III_{Q_o} and genetic manipulations of complex III activity, has led to speculation that superoxide production from site III_{Q_o} plays an important role in cellular signaling during

hypoxia and other events [19–21]. However, this conclusion remains controversial [22]. Unfortunately, because of the intimate links between ROS production, redox signaling and broader metabolism there is no definitive evidence for a direct link between any of these sites of superoxide/H₂O₂ production and a particular physiologically-relevant condition.

Antioxidants have been instrumental in the development of theories regarding the physiological roles of ROS. Antioxidant research has yielded thousands of natural and man-made chemicals and numerous gene products that broadly modulate ROS with differing selectivity and potency and within different cellular compartments. While antioxidants generally do not interfere with electron transport or oxidative phosphorylation, they scavenge ROS downstream from production and therefore can never fully suppress the effects of ROS. In addition, although ROS have been implicated in numerous disease states and antioxidants have shown promise in many pre-clinical experiments, virtually all clinical trials of antioxidant-based therapeutics have shown limited efficacy [23–25]. Therefore, from a fundamental understanding of the mechanisms of ROS production to the development of effective therapeutics, there remains a pressing need to identify the ways in which mitochondrial superoxide/H₂O₂ production is involved in (patho)physiological processes as well as the means by which this production can be modulated selectively.

Toward both of these ends, we developed a panel of high-throughput assays for the identification of compounds that modulate superoxide/H₂O₂ production at defined sites in isolated mitochondria without concomitant changes in energy metabolism. Our unbiased approach efficiently identifies site-specific modulators of superoxide/H₂O₂ production while also revealing less-specific effectors such as broad-acting antioxidants and novel inhibitors of mitochondrial function. We describe, for the first time, a site-selective inhibitor of mitochondrial superoxide/H₂O₂ production that does not compromise normal mitochondrial function. This novel inhibitor, CN-POBS, suppresses the majority of superoxide/H₂O₂ production from site I_Q without altering superoxide/H₂O₂ production at other sites and without affecting mitochondrial energetic status. Our screening strategy represents a significant advance in the ability to discover small molecules with potent and selective effects on mitochondrial electron flow while our novel inhibitors promise to advance our understanding of the mechanisms of mitochondrial ROS production in more complex systems.

Experimental procedures

Reagents, animals, mitochondrial isolation, and standard buffers

CaCl₂ standard was from Thermo Scientific. Amplex UltraRed and tetramethylrhodamine methyl ester (TMRM) were from Invitrogen. Compounds for screening were from a diverse, non-combinatorial library obtained from ChemBridge. New stocks of primary hits and their structural analogs were also from ChemBridge. The biological activity of N-cyclohexyl-4-(4-nitrophenoxy)benzenesulfonamide, CN-POBS, obtained from ChemBridge (ID 5229982) was validated using compound obtained from ChemDiv (ID 0668-0074) and found to be essentially identical. All other reagents were from Sigma-Aldrich.

Skeletal muscle mitochondria were isolated from hindlimbs of 5–8 week old female Wistar rats (Harlan Laboratories) as previously described [26]. The animal protocol was approved by the Buck Institute Animal Care and Use Committee, in accordance with IACUC standards.

Unless stated otherwise, freshly isolated muscle mitochondria were assayed in KHEB medium containing 120 mM KCl, 5 mM HEPES, 1 mM EGTA and 0.3% (w/v) bovine serum albumin. Where indicated, total and free calcium concentrations in assay buffers were calculated using the Extended MaxChelator program available at <http://maxchelator.stanford.edu>.

Screen for site-selective inhibitors of mitochondrial H₂O₂ production

Screening—To screen for site-selective small-molecule inhibitors of mitochondrial H₂O₂ production, we designed a core set of five assays using distinct combinations of substrates and inhibitors of electron transport (Fig. 1). Assays were performed in parallel and differed only in the amount of mitochondria and the substrates and inhibitors used. Superoxide and H₂O₂ were measured fluorometrically as H₂O₂ without distinguishing between them, in the presence of exogenous superoxide dismutase (25 U • mL⁻¹), horseradish peroxidase (1 U • mL⁻¹), and Amplex UltraRed (25 μM) as described [26] except assays were performed in 96-well format at room temperature (about 21 °C). Compounds that generally inhibited mitochondrial function were filtered with a sixth assay, of mitochondrial membrane potential (Ψ_m) using the potentiometric dye TMRM.

The screening workflow is shown in Fig. 2A. 3,200 compounds (~10 mM in DMSO) were arbitrarily selected from a library of 24,000 compounds obtained from ChemBridge. Master screening plates each with 80 compounds were prepared and diluted with KHEB medium using a Biomek FX liquid handling workstation (Beckman) just prior to screening (final testing concentration ~2.5 μM). On each master plate, eight DMSO wells (negative controls) were evenly distributed in the first and last columns of wells. Eight wells on each plate were reserved for duplicates of four known mitochondrial inhibitors (positive controls; their effect is reflective of a “positive” hit in certain designated assays), prepared fresh in KHEB. Final concentrations were: 1 μM carbonylcyanide-4-(trifluoromethoxy)phenylhydrazone (FCCP), a chemical uncoupler used as a positive control for site I_Q superoxide production and the assay of Ψ_m; 2 μM myxothiazol, a potent inhibitor of site III_{Q₀} and positive control for site III_{Q₀} superoxide production; 1 mM malonate, a competitive inhibitor of complex II and positive control for the superoxide/H₂O₂ production by the flavin binding site of complex II (site II_F); 20 mM aspartate, a substrate for aspartate aminotransferase that removes matrix 2-oxoglutarate to act as a positive control for superoxide/H₂O₂ production from site I_F plus NADH-linked matrix dehydrogenases including 2-oxoglutarate dehydrogenase and pyruvate dehydrogenase (collectively site I_F/DH) [16].³

The mitochondrial suspension and a solution of Amplex UltraRed with superoxide dismutase and horseradish peroxidase were diluted in KHEB just prior to use. Sites of mitochondrial superoxide/H₂O₂ production were targeted individually using different

³C. L. Quinlan, M. H. Mogensen, R. L. S. Goncalves, V. I. Bunik, M. D. Brand, Manuscript in preparation.

combinations of mitochondrial substrates and inhibitors (Fig. 2A). These different “Start Solutions” were designed to generate maximal rates of H₂O₂ production predominantly from a single site within the chain. The sites of production targeted [15, 16] and the Start Solutions used to stimulate H₂O₂ production during screening were: site I_Q with 5 mM succinate; site I_F/DH with 5 mM glutamate, 5 mM malate and 4 μM rotenone; site III_{Q₀} with 5 mM succinate, 4 μM rotenone and 2.5 μM antimycin A; site II_F with 15 μM palmitoylcarnitine, 2.5 μM antimycin A and 2 μM myxothiazol; mGPDH with 25 mM glycerol phosphate, 4 μM rotenone, 2.5 μM antimycin A, 1 mM malonate and 2 μM myxothiazol (Fig. 1). A Biomek FX workstation was used to dispense all components into black 96-well assay plates. The addition of the Start Solutions initiated each assay. Plates were incubated in the dark at room temperature (about 21 °C) for 30 – 40 min and endpoint fluorescence was measured on a Victor 3V plate reader (Perkin Elmer) equipped with a λ_{ex} 550 nm/λ_{em} 590 nm filter cube.

Ψ_m was assayed manually by transferring diluted compounds to black 96-well assay plates. A bulk solution was prepared containing the following components and dispensed into two assay plates (all concentrations final): 0.2 mg protein • mL⁻¹ mitochondria, 5 μM TMRM, 5 mM glutamate, 5 mM malate and 80 ng • mL⁻¹ of the K⁺/H⁺ exchanger nigericin to collapse the pH gradient across the inner membrane (ΔpH) and maximize Ψ_m. Assay plates were incubated in the dark at room temperature (about 21 °C) for 10 – 15 min and endpoint fluorescence was measured on a Victor 3V plate reader equipped with a λ_{ex} 550 nm/λ_{em} 590 nm filter cube.

Hit selection—Endpoint fluorescence values were scaled as % change from the average of eight intra-plate DMSO negative control wells, with the duplicate wells containing the relevant positive control inhibitor defined as –100% (see “Screening” for the assignment of inhibitors to each assay). Values for the mGPDH superoxide/H₂O₂ assay were arbitrarily scaled to the values for FCCP wells in the parallel site I_Q H₂O₂ assay since no potent and selective inhibitors of mGPDH superoxide/H₂O₂ production existed at the start of this project [27]. Subsequently, this decision to use the FCCP values from the site I_Q superoxide/H₂O₂ assay was found to underestimate the potency of compounds against mGPDH-specific H₂O₂ production. However, we maintained this procedure throughout the screen for consistency and lowered the threshold for hit identification in the mGPDH assay accordingly.

Following initial scaling, normalized intra-plate values were subjected to Tukey’s two-way median polish to remove row- and column-dependent positional effects [28, 29]. Initially, hits in each H₂O₂ assay were identified by applying a threshold of at least a 20% decrease in that assay. A critical component of the procedure was the use of two-tiered filtering for non-specific hits. First, each H₂O₂ assay was used to counterscreen each of the other H₂O₂ assays. This parallel counterscreening eliminated the vast majority of non-selective modulators of H₂O₂ production or consumption as well as compounds that produced artifacts in the detection system such as fluorescence quenching or interference with the HRP-Amplex UltraRed reaction. A smaller set of non-selective modulators or general inhibitors of mitochondrial function was flagged at the second step using the Ψ_m counterscreen. Most frequently, the Ψ_m assay eliminated marginal compounds or those

structurally related to more potent inhibitors of Ψm . Hits in a single assay at the -20% threshold were subsequently eliminated if they altered the other H_2O_2 or Ψm assays by more than 10% or 4% , respectively. Based on the final number of hits in each assay, consideration of structural similarities among hits, and consideration of the underestimation in the mGPDH assay mentioned above, the thresholds for inclusion for the site $\text{I}_\text{F}/\text{DH}$ and mGPDH assays were adjusted to -18% and -10% , respectively, to generate additional hits for further testing. $2 - 6\%$ of tested compounds surpassed the threshold in a given assay, but, after the two-tiered elimination process, only $0.1 - 0.5\%$ were retained as potent and selective hits.

Retesting against an expanded panel of superoxide/ H_2O_2 and Ψm assays

Hits from the primary screen and selected structural analogs were sourced from ChemBridge and retested against an expanded set of site-specific H_2O_2 and Ψm assays. Important changes from the original screen were as follows: four compounds were titrated in duplicate between $0.08 - 80 \mu\text{M}$ on each 96-well plate and a total of 32 DMSO controls were interspersed across each plate to serve as local normalization controls in place of two-way median polishing. Two additional H_2O_2 assays were included for all retesting: site I_Q with 0.5 mM succinate, and site III_Q_0 with 0.5 mM succinate, $4 \mu\text{M}$ rotenone and $2.5 \mu\text{M}$ antimycin A. For retesting certain inhibitors of site I_Q H_2O_2 production, an assay containing 5 mM succinate and 0.5 mM glutamate was also included. On select plates, FCCP ($0.0025 - 2.5 \mu\text{M}$) or rotenone ($0.02 - 20 \mu\text{M}$) was included for comparison to candidate inhibitors of site I_Q H_2O_2 production. Ψm was assayed manually in four different conditions: 5 mM glutamate and 5 mM malate; 5 mM glutamate, 5 mM malate and $80 \text{ ng} \cdot \text{mL}^{-1}$ nigericin; 5 mM succinate and $4 \mu\text{M}$ rotenone; 5 mM succinate, $4 \mu\text{M}$ rotenone and $80 \text{ ng} \cdot \text{mL}^{-1}$ nigericin.

Hit validation—Endpoint fluorescence values were scaled to intra-plate DMSO and positive control inhibitor wells as described in “Hit Selection” except that the median values for interspersed DMSO wells (3 – 6 nearest DMSO wells for each compound well) were used as negative control values rather than only the eight DMSO wells in columns 1 and 12. This method replaced the two-way median polish used during high-throughput screening but had the similar effect of minimizing positional row and column effects in low signal:noise assays. Hits were validated if they caused progressive, dose-dependent inhibition of H_2O_2 production from a single site over at least a 5 – 10 fold concentration range without strong effects on other sites of H_2O_2 production or the maintenance of Ψm . At this stage, strong candidates were not necessarily excluded from further testing if subtle off-target effects were observed (e.g. loss of specificity or signs of general inhibition at the highest concentrations). Often, these candidates were pursued for more detailed mechanistic studies with the expectation that subsequent structure-activity analysis would yield structurally-related compounds with better selectivity.

Steady-state measurements of NAD(P)H, cytochrome b_{566} , H_2O_2 production and Ψm

Steady-state % reduction levels of NAD(P)H and cytochrome b_{566} were determined as described in [15]. Steady-state rates of H_2O_2 production were measured using Amplex UltraRed in a Varian Cary Eclipse fluorimeter as described in [26]. Although no effect of

CN-POBS on the HRP-Amplex UltraRed detection system was observed, H₂O₂ calibration curves were always generated in the presence and absence of CN-POBS and applied as appropriate. Steady-state Ψ_m was calibrated using an electrode sensitive to the cation methyltriphenylphosphonium (TPMP) in the absence or presence of 80 ng • ml⁻¹ nigericin as described in [15, 26]. The effect of CN-POBS on steady-state variables was tested at 37 °C with continuous stirring in either KHEB or KHEB plus 5 mM KH₂PO₄ and 2.5 mM MgCl₂.

Measurement of the rate of reverse electron transport

Dose-dependent effects of CN-POBS, FCCP or rotenone on the rate of reverse electron transport from succinate to NAD(P)⁺ was measured using a Varian Cary Eclipse fluorimeter with minor changes to previous procedures [30]. Briefly, to fully activate complex II and obtain maximal rates of NAD⁺ reduction, mitochondria (0.3 mg protein • mL⁻¹) were equilibrated in KHEB medium for 15 s at 37 °C with continuous stirring then 0.5 mM glutamate was added to facilitate conversion of oxaloacetate to aspartate by aspartate aminotransferase. After another 15 s, 5 mM succinate was added and the immediate, rapid rate of NAD(P)⁺ reduction was measured. Rates of NAD(P)⁺ reduction were calculated as % of vehicle control (DMSO for CN-POBS and rotenone, ethanol for FCCP).

Measurement of respiration

The effect of candidate compounds on basal state 2 (substrate only), phosphorylating state 3 (5 mM ADP) and non-phosphorylating state 4o (0.5 ug • mL⁻¹ oligomycin) were measured in plate-attached skeletal muscle mitochondria using a Seahorse XF24 Analyzer according to [27, 31]. Compounds were added just prior to loading the assay plate into the instrument. Each concentration of compound was tested in at least two wells on each plate. At least three biological replicates of each titration in each substrate condition were performed. Measurements were performed in a mannitol- and sucrose-based medium (Seahorse MAS buffer [31]) containing 0.3% (w/v) bovine serum albumin and 1 mM EGTA without or with 250 nM free calcium at pH 7.0.

Data presentation and statistical analysis

Data are presented as mean ± SE except screening data where error bars represent ranges of duplicate values. Statistical differences between conditions were determined with GraphPad Prism software using Student's *t*-test, one-way ANOVA with Newman-Keuls post-test, or two-way ANOVA with Bonferroni post-test as specified in the Figure legends. *p* values < 0.05 were considered significant.

Results and Discussion

Unbiased profiling for site-selective inhibitors of mitochondrial H₂O₂ production

Our goal was to discover compounds that suppress the leak of electrons onto oxygen that occurs from multiple sites within mitochondria. Importantly, we desired compounds that act in a site-selective manner and without altering the normal electron and proton fluxes that drive mitochondrial oxidative phosphorylation. To accomplish this goal we designed a set of microplate-based assays to monitor H₂O₂ production from five distinct sites along with an

assay to monitor Ψ_m . Five sites of H_2O_2 production were targeted separately by adding to a common assay mixture different substrates without or with selected inhibitors (Fig. 2A). In parallel, a distinct counterscreen to monitor Ψ_m was used to eliminate compounds that were likely general inhibitors of the electron transport chain or uncouplers of mitochondrial ATP production (rightmost assay, Fig. 2A). Each assay was robust, with Z-factors [32] above 0.5, and all but one assay had a coefficient of variation below 5% (Table 1). The combination of this robustness and our use of five separate counterscreens for each assay of H_2O_2 production resulted in an efficient platform for identifying site-selective inhibitors of superoxide/ H_2O_2 production. Of 3200 compounds tested in our primary screening, approximately 2 – 6% had a strong effect on a given assay. For example, for the assay of superoxide/ H_2O_2 production at site I_Q , 180 compounds (5.6% of total) surpassed the threshold of –20% designated for this assay (gray circles below dashed line in Fig. 2B). However, when each of these compounds was crosschecked for effects on any of the other four sites of superoxide/ H_2O_2 production or in the Ψ_m assay, only 13 compounds remained (red circles in Fig. 2B – 2G; 0.4% of total). These 13 compounds represented the initial leads in our search for site-selective inhibitors of superoxide/ H_2O_2 production from site I_Q . In comparison, between four and 17 site-selective hits were identified for the other four sites of superoxide/ H_2O_2 production (Table 1).

Next, we retested many of the 55 site-selective compounds against an expanded panel of H_2O_2 and Ψ_m assays (see "Experimental procedures" for specific conditions) to verify their selectivity and to begin to probe for mechanisms of action. The I_F/DH , III_{Q_0} , and mGPDH assays all yielded one or more structural classes of novel inhibitors of superoxide/ H_2O_2 production from these sites to be described in detail elsewhere. Briefly, the majority of these compounds validated the results of our primary screen under the conditions tested. However, the hits in these assays were ultimately found to have condition-dependent effects on H_2O_2 production or substrate oxidation. For example, inhibitors in the assay of mGPDH superoxide production were found to inhibit mGPDH enzymatic activity in more detailed follow-up experiments [27].

The assay for I_Q superoxide/ H_2O_2 production had the highest Z-factor and lowest CV of the five H_2O_2 assays used in the primary screen and yielded 13 compounds that were selective inhibitors for this site of superoxide/ H_2O_2 production (Table 1). Among these 13 were several structurally-similar compounds, the most potent of which was CN-POBS.

Validating inhibitors of site I_Q superoxide/ H_2O_2 production

To verify the activity of these compounds, we generated dose-response curves between 0.08 and 80 μM against our panel of H_2O_2 and Ψ_m assays for several of the 13 original hits and over 20 structurally-related compounds available through ChemBridge. To better compare the selectivity of these I_Q superoxide/ H_2O_2 inhibitors, we first estimated their IC_{50} against superoxide/ H_2O_2 production from site I_Q with 5 mM succinate. We then determined the % change in H_2O_2 or Ψ_m signal in the other assays at these concentrations (Table 2).

Two of the most potent hits in the original screen, compounds **1** and **2**, remained potent inhibitors of site I_Q superoxide/ H_2O_2 production with 5 mM succinate. However, **1** gave slight inhibition of site I_F/DH H_2O_2 production at 2.5 μM as well as a subtle inhibition of

succinate oxidation revealed by differing effects on site III_{Qo} superoxide production that were dependent upon the concentration of succinate (data not shown). Specifically, it caused a dose-dependent decrease in superoxide production from site III_{Qo} driven by 0.5 mM succinate, but increased superoxide production from the same site when driven by 5 mM succinate. In the absence of Ψ_m , superoxide production from site III_{Qo} peaks at an intermediate reduction state of the ubiquinone pool [33]. Our assays for superoxide production from site III_{Qo} were designed to target both the peak rate of production with 0.5 mM succinate and a lower, but significant rate near complete reduction of the ubiquinone pool with 5 mM succinate. The effects of **1** were best explained by an inhibition of succinate oxidation that progressively lowered the reduction state of the ubiquinone pool causing a drop from the peak of the curve with 0.5 mM succinate and an increase toward the top of the peak with 5 mM succinate. Low concentrations of malonate can cause a similar effect [33].

Compound **2** likely also inhibited succinate oxidation or uptake. Its effects on site III_{Qo} superoxide production were more potent than **1** in that it fully inhibited III_{Qo} superoxide production driven by low succinate below 8 μ M whereas **1** inhibited only ~50% at 80 μ M. Between 0.08 – 0.8 μ M, **2** increased site III_{Qo} superoxide production with high succinate but progressively and completely inhibited this production by 80 μ M. Again, these effects were best explained by a progressive inhibition of succinate uptake or oxidation that lowered the reduction state of the ubiquinone pool driven by succinate. Further support for this explanation came from the observations that superoxide/H₂O₂ production from site I_Q was more sensitive to **2** when driven by 0.5 mM succinate than with 5 mM succinate and that Ψ_m driven with succinate was more sensitive than Ψ_m driven with glutamate and malate (data not shown). Evidence to support an effect on succinate uptake rather than a direct effect on oxidation at complex II was the fact that site II_F superoxide/H₂O₂ production driven by palmitoylcarnitine was inhibited only ~30% at 80 μ M **2** (data not shown). Interestingly, the effect of **2** on site III_{Qo} superoxide production with 5 mM succinate was not detected in the original screen because the inflection point caused by **2** in the signal of this assay occurred near the screening concentration of 2.5 μ M. Therefore, it showed no change in H₂O₂ signal relative to DMSO controls at this concentration but greatly increased or decreased H₂O₂ signal at lower or higher concentrations, respectively. Together, these results emphasize the effectiveness of the primary screen to reveal novel modulators of mitochondrial function and the efficiency with which our retesting strategy could both eliminate false positives and provide useful information on mechanisms of action of novel modulators.

Two compounds, **3** and **4**, did not reach the threshold of –20% set for the I_Q H₂O₂ assay, but shared structural similarity and were therefore selected for further testing (Table 2). As in the primary screen, these compounds were less potent against I_Q superoxide/H₂O₂ production (IC₅₀ ~25 μ M). However, at this concentration both compounds inhibited site II_F superoxide/H₂O₂ production driven with palmitoylcarnitine, although they had no significant effects on site III_{Qo} superoxide production with either low or high succinate (data not shown and Table 2). Therefore, these compounds appeared to have off-target effects involving fatty acid oxidation. Further evaluation of structurally similar compounds may reveal if the dual effects of this class of compound are separable.

Most of the other compounds tested for selectivity against I_Q superoxide/H₂O₂ production were members of a structural class exemplified by the most potent and selective hit identified in the primary screen, CN-POBS (Table 2). This class was characterized by a core 4-phenoxy-benzenesulfonamide "POBS" structure. A comparison of multiple members of this class revealed structural features that were important for selectivity against I_Q superoxide/H₂O₂ production. Three compounds (**6**, **7** and **10**) were more potent against I_Q superoxide/H₂O₂ production than CN-POBS, with IC₅₀ < 1 μM, and differed structurally only in substitutions at the terminal nitrogen in the sulfonamide group. Specifically, while CN-POBS has a cyclohexyl group on the terminal nitrogen, these three compounds have benzene rings with additional sizable or electron-withdrawing groups. Several other compounds with similar substitutions were also tested (data not shown). Commonly, these compounds had a greater effect on site II_F superoxide/H₂O₂ production at or just above their IC₅₀ (Table 2 and data not shown) than did CN-POBS, which affected site II_F superoxide/H₂O₂ production driven by palmitoylcarnitine only at the highest concentrations tested (Fig. 3). Notably, as observed for **3** and **4**, this effect was likely due to inhibition of fatty acid oxidation and not complex II because CN-POBS did not inhibit superoxide/H₂O₂ production from site II_F when driven by succinate (data not shown). It is possible that these compounds interfered with palmitoylcarnitine transport or metabolism and that the terminal group off the sulfonamide modulated this off-target effect. In addition, some compounds more strongly inhibited the reverse flux of electrons from succinate to NAD(P)⁺ via complex I at their IC₅₀ than did CN-POBS (rightmost column in Table 2). Other structural modifications decreased potency, selectivity, or both. Selected examples of these modifications and their effects on site-specific superoxide/H₂O₂ production and Ψ_m are provided in Table 2 (compounds **6** – **15**).

Importantly, our retesting strategy identified CN-POBS as the most potent and selective inhibitor of site I_Q superoxide/H₂O₂ production among the compounds tested. All further experiments focused on characterizing the effects of this novel inhibitor in more detail.

CN-POBS is a novel site-selective inhibitor of superoxide/H₂O₂ production from site I_Q

Dose-response curves for CN-POBS against the expanded panel of site-specific superoxide/H₂O₂ assays are shown in Fig. 3. CN-POBS showed remarkable selectivity for superoxide/H₂O₂ production from site I_Q. No significant effects on H₂O₂ production were observed below 25 μM for any of the other four sites tested.

CN-POBS slightly, but consistently, inhibited H₂O₂ production driven by saturating succinate more potently than H₂O₂ production driven by subsaturating succinate (compare white and black squares in Fig. 3). This difference was likely due to superoxide/H₂O₂ production from sites other than I_Q during oxidation of succinate alone [16]. Succinate oxidation increases the reduction state of both the NADH pool in the matrix and the ubiquinone pool of the inner membrane and induces superoxide/H₂O₂ production from site I_F/DH and site III_{Q_o}, respectively [9, 15, 33]. In the presence of subsaturating succinate, site II_F may also be active [15]. Depending on the relative protonmotive forces, relative reduction states of the redox centers, and the contribution from site II_F with either high or low succinate, it is possible that the relative contribution of these sites to the total signal

versus the contribution from site I_Q may be greater with subsaturating succinate. Such a shift in the sources of production would lower the relative effect of CN-POBS on total H₂O₂ production under this condition. Importantly, this relative effect is the opposite of what was observed for novel and known inhibitors of succinate oxidation as described in “Validating inhibitors of site I_Q superoxide/H₂O₂ production” above. For these compounds, superoxide/H₂O₂ production with low succinate was *more* sensitive than with high succinate alone. This distinction argues against inhibition of succinate oxidation as a likely mechanism of action for CN-POBS.

To further evaluate the selectivity of CN-POBS for effects on electron leak to oxygen at site I_Q and not on electron flow through the electron transport chain, we measured Ψ_m (Fig. 4A) and respiration (Fig. 4B) with different substrates and energetic conditions. CN-POBS had no effect on succinate or glycerol 3-phosphate oxidation below the highest concentration tested, 80 μ M. However, there was a significant effect of CN-POBS on Ψ_m (at 8 μ M) and respiration (at 80 μ M) powered by the complex I substrates glutamate plus malate. The greater potency of CN-POBS in the TMRM-based Ψ_m assays *versus* the respiration measurements driven with glutamate and malate was subsequently identified as a sensitizing effect of 5 μ M TMRM specifically during oxidation of glutamate and malate (data not shown). Similar inhibitory effects of TMRM on respiration driven by glutamate plus malate have been shown previously [34]. To confirm that CN-POBS had no off-target effects on substrate oxidation at concentrations near its IC₅₀, we also measured Ψ_m using an electrode sensitive to the potentiometric cation TPMP. We observed no effect of 2.5 μ M CN-POBS on Ψ_m powered by either glutamate plus malate or succinate either in the presence or absence of the K⁺/H⁺-exchanger nigericin (Table 3).

Together, these data indicate that CN-POBS can suppress at least 50% of superoxide/H₂O₂ production from site I_Q without any effects at other sites of H₂O₂ production, on generation of protonmotive force, or on oxidative phosphorylation.

CN-POBS lowers superoxide/H₂O₂ production at site I_Q without inhibiting electron flux through complex I

The superoxide/H₂O₂ production that we attribute to site I_Q is best associated with reverse electron transport and is dependent on the normal kinetic mechanisms of electron flux and proton pumping of complex I [35]. Reverse electron transport will also cause the FMN at site I_F to become reduced and generate superoxide [35, 36]. Therefore, it is possible that the suppression of superoxide/H₂O₂ associated with reverse electron transport observed with CN-POBS is due to an impairment in flux through complex I. Such an impairment would decrease superoxide/H₂O₂ production at both sites. To determine if the inhibition of superoxide/H₂O₂ production associated with reverse electron transport by CN-POBS was due to altered kinetics of complex I, we measured the rate of NAD(P)⁺ reduction from succinate *via* complex I. A dose-response curve showed that CN-POBS had no significant effect on reverse electron flux through complex I below 25 μ M (Fig. 5A) although it significantly decreased H₂O₂ production at every concentration tested between 0.25 and 80 μ M (Fig. 5B). A correlation plot of the relative effects on the rate of NAD(P)⁺ reduction *versus* the rate of H₂O₂ production confirmed that at least 50% of superoxide/H₂O₂

production was suppressed by CN-POBS with no effect on the flux through complex I (Fig. 5C).

Other known inhibitors of superoxide/H₂O₂ production during reverse electron transport act by inhibiting electron transport through site I_Q (e.g. rotenone), by dissipating the protonmotive force that drives reverse electron transport (e.g. FCCP), or by inhibiting oxidation of the substrate providing electrons to site I_Q (e.g. malonate during succinate oxidation). Our data ruled out a direct effect on succinate oxidation by CN-POBS below 80 μM (see above and Figs. 3, 4A, 4B). To test the other two mechanisms, we compared the rates of NAD(P)⁺ reduction and H₂O₂ production during succinate oxidation in the presence of differing amounts of rotenone or FCCP. As expected, each potentially inhibited both the rate of NAD(P)⁺ reduction *via* complex I (Fig. 5A) and the rate of H₂O₂ production (Fig. 5B). However, FCCP was not able to dissociate these effects, and only the lowest concentration of rotenone (20 nM) lowered H₂O₂ production with a small but not significant decrease in the rate of NAD(P)⁺ reduction (Fig. 5C). In comparison, CN-POBS had a much broader window of differential effects.

We conclude that CN-POBS suppresses superoxide/H₂O₂ production by a unique mechanism that is independent of altered flux through complex I and is therefore best described as acting at site I_Q. Because CN-POBS is lipophilic (logP = 4.1), we speculate that it may interact with specificity near site I_Q in the hinge region connecting the membrane-associated domains to the soluble subunits in the matrix. At high concentrations, the lipophilicity of CN-POBS may promote non-specific interactions with other membrane-associated domains like the proton pumping channels to fully inhibit the complex.

CN-POBS suppresses two-thirds of superoxide/H₂O₂ production at site I_Q without changes in other mitochondrial functions

As mentioned above, multiple sites of superoxide/H₂O₂ production are active during oxidation of succinate alone [16]. Because other sites of H₂O₂ production are unaffected by CN-POBS below 25 μM (Fig. 3), their contribution to the total H₂O₂ production may cause an underestimation of the effect of CNPOBS on site I_Q superoxide/H₂O₂ production with succinate alone. To more accurately determine the potency of CN-POBS against superoxide/H₂O₂ production at site I_Q, we determined the effect of CNPOBS on calibrated steady-state rates of H₂O₂ production driven by succinate alone without and with complex I activity fully inhibited by rotenone. First, to verify that CN-POBS was without effect on various aspects of oxidative phosphorylation, we measured the reduction states of NAD(P)H and ubiquinone and the value of Ψ_m after addition of succinate. CN-POBS had no effect on any of these variables (Table 3). However, it significantly lowered the rate of H₂O₂ production measured under the same conditions by 50% (Fig. 6A). Using rotenone to fully block site I_Q resulted in a significantly larger decrease in the total rate of H₂O₂ production from succinate than observed with CN-POBS and succinate alone. However, CN-POBS had no additional effect in the presence of rotenone (Fig. 6A). The addition of rotenone to mitochondria oxidizing succinate can change the distribution of electrons at superoxide/H₂O₂-producing redox centers such as site I_F/DH and site III_{Q_o} [16]. Therefore, it is important to account for changes in superoxide/H₂O₂ production at these sites prior to

assignment of the entire rotenone-sensitive component to site I_Q. This correction is made using the reduction states of the matrix NAD(P)H signal and cytochrome *b*₅₆₆ signal in complex III to determine the relative rates of superoxide/H₂O₂ production that are produced by site I_F/DH and site III_{Q_o}, respectively [15, 16]. We observed no significant difference in either the % reduction of NAD(P)H or % reduction of cytochrome *b*₅₆₆ with the addition of rotenone to succinate (Table 3). Therefore, in this particular case, the rotenone-sensitive component of the H₂O₂ production accurately described the rate attributable to site I_Q. The site I_Q-specific rate of H₂O₂ production with succinate alone was 1144 ± 86 pmol • min⁻¹ • mg protein⁻¹ (n = 3). In comparison, the amount sensitive to 2.5 μM CN-POBS was 762 ± 69 pmol • min⁻¹ • mg protein⁻¹ (n = 3). Therefore, CN-POBS selectively suppressed 67% of the H₂O₂ production from site I_Q without altering H₂O₂ production from at least five other major sites of mitochondrial superoxide/H₂O₂ production (sites I_F/DH, II_F, III_{Q_o}, and mGPDH) and without affecting any measured aspect of mitochondrial activity including oxidation of fatty-acyl carnitine, basal and phosphorylating respiration, protonmotive force (Ψ_m or pH), electron flux through complex I, and the reduction states of the NAD(P)H and ubiquinone pools. This represents the first identification of such a site-selective inhibitor of mitochondrial superoxide/H₂O₂ production without effects on oxidative phosphorylation. Previous studies [30] identified diphenyleneiodonium as an inhibitor of superoxide/H₂O₂ production from site I_Q, but not site I_F/DH or site III_{Q_o}. However, this compound has strong off-target effects on oxidative phosphorylation, greatly limiting its utility.

The hypothesis that complex I has two distinct sites of superoxide/H₂O₂ production (site I_F and site I_Q) rather than a single site (I_F) activated under different conditions, remains a subject of debate [9, 36]. Although our data indicates no effect of CN-POBS on superoxide production by site I_F/DH, our screening assays were not designed to distinguish between superoxide/H₂O₂ production from site I_F and superoxide/H₂O₂ production from matrix dehydrogenases, and may not have been sensitive enough to detect subtle effects specifically on site I_F. Therefore, we tested the effect of CN-POBS under conditions in which site I_F is the sole producer of superoxide.³ In agreement with our screening data, CN-POBS had no effect on superoxide/H₂O₂ production specifically from site I_F (Fig. 6B). Therefore, our discovery of CN-POBS provides strong support for the existence of two sites of superoxide/H₂O₂ production in complex I, as it significantly inhibits superoxide/H₂O₂ production associated with reverse electron transport into site I_Q but has no effect on reverse electron transport to site I_F, on steady-state NAD(P)H reduction, or superoxide/H₂O₂ production under any conditions in which site I_F is expected to be active.

Site I_Q does not produce significant amounts of superoxide/H₂O₂ during forward flux of electrons through complex I

In isolated mitochondria, site I_Q has a high capacity for superoxide/H₂O₂ production during the oxidation of substrates such as succinate and glycerol 3-phosphate that directly reduce ubiquinone and generate a large enough protonmotive force to drive electron transport in reverse into complex I [16, 18]. In intact cells, it remains unclear how much site I_Q contributes to superoxide/H₂O₂ production under conditions that strongly favor forward electron flux through complex I. Recently, through the use of endogenous reporters of site I_F/DH and site III_{Q_o}, we demonstrated that these sites account for all of the measured H₂O₂

production under several conditions [15]. However, during non-phosphorylating oxidation of glutamate plus malate, a significant portion of the measured H₂O₂ production could not be attributed to site I_F/DH and site III_Q. Of the conditions tested, this had the highest membrane potential and reduction state of the ubiquinone pool, conditions that favor superoxide/H₂O₂ production from site I_Q. Therefore, to determine if site I_Q contributed significantly to the total rate of H₂O₂ production under this condition, we repeated these measurements of calibrated rates of H₂O₂ production, Ψ_m , % reduction of NAD(P)H, and % reduction of cytochrome *b*₅₆₆ in both the absence and presence of CN-POBS. As observed under other conditions, 2.5 μ M CN-POBS did not alter Ψ_m or the reduction state of either redox pool (Table 3). In calibrated measurements of H₂O₂ production, CN-POBS had no significant effect on the total rate of production (Fig. 7). Although CN-POBS caused small (2 – 7%) decreases in total H₂O₂ production in three out of four trials, the average effect was non-significant at $-2.5 \pm 2.0\%$ (n = 4). With the additional consideration that CN-POBS suppresses only 67% of site I_Q superoxide/H₂O₂ production at 2.5 μ M (see previous section), the potential maximal contribution of site I_Q likely was still less than 4%. Therefore, we conclude that site I_Q is not a significant source of superoxide/H₂O₂ production under these conditions. This exclusion leaves open the idea that the source of the unattributed H₂O₂ production is likely 2-oxoglutarate dehydrogenase [16]³.

It is important to note that the absence of superoxide/H₂O₂ production from site I_Q during oxidation of glutamate plus malate in isolated mitochondria does not rule out a role for site I_Q superoxide/H₂O₂ production under other conditions in which the matrix NADH pool is reduced and there is forward electron flux through complex I (e.g. in intact cells respiring on glucose or fatty acids). Indeed, the rate of H₂O₂ production in isolated mitochondria metabolizing succinate alone is stimulated by additional substrates that reduce matrix NAD⁺, such as glutamate, 2-oxoglutarate, pyruvate and palmitoylcarnitine [37]. In uninhibited systems, the rate of H₂O₂ production and the participation of different sites depend on the substrates being oxidized [16]. Therefore, context-dependent shifts in the sizes of different substrate pools along with changes in energetic demand will determine the contribution of site I_Q in more complex systems. For example, there is evidence that increased flux through mGPDH drives superoxide/H₂O₂ production at site I_Q during T-cell activation [38]. In a pathological context, a role for site I_Q superoxide/H₂O₂ production may be most likely during reperfusion after ischemic events. During ischemia, succinate levels rise significantly and remain elevated after reperfusion [39, 40]. Therefore, it is possible that site I_Q contributes to the burst of superoxide/H₂O₂ production on reperfusion [41]. A potential role for site I_Q superoxide/H₂O₂ production during reperfusion is supported by recent observations that a cysteine residue adjacent to site I_Q is selectively nitrosylated during ischemia and that this modification protects against ROS production and tissue damage induced by subsequent reperfusion [42]. Interestingly, inhibition of complex I with pyridaben significantly attenuated, and inhibition of complex II with 3-nitropropionic acid significantly exacerbated, tissue damage caused by ischemia/reperfusion in neonatal mice [43]. Because these inhibitors may alter Ψ_m , rates of ATP synthesis, and electron distribution at multiple sites including site I_Q, it would be interesting to repeat these effects in the presence of CN-POBS to determine more directly whether site I_Q superoxide/H₂O₂ production plays a significant role in ischemia/reperfusion injury.

Conclusions

Previous strategies to address questions of mitochondrial superoxide/H₂O₂ production involved acute pharmacological intervention with potent inhibitors of mitochondrial activity, longer-term molecular suppression of gene products that invariably alter normal mitochondrial metabolism, or chemical or enzymatic antioxidants that act downstream of production in a relatively non-specific manner and often indirectly influence cellular redox balance. The use of site-selective inhibitors of superoxide/H₂O₂ production that do not impair mitochondrial function allows more direct testing of hypotheses regarding the mechanisms of superoxide/H₂O₂ production, the contributions of distinct sites to overall production in complex systems, and the (patho)physiological consequences of production from specific sites in intact systems. As the first known site-selective inhibitor of superoxide/H₂O₂ production that does not interfere with oxidative phosphorylation, CN-POBS provides a proof-of-concept that such molecules exist. Despite the observed lack of a significant contribution from site I_Q to the total H₂O₂ production during oxidation of glutamate plus malate, our ability to address this hypothesis using a site-selective inhibitor of superoxide/H₂O₂ production that does not interfere with normal mitochondrial energetics represents a fundamental shift in the approach to questions of mitochondrial ROS production. In addition, our efficient and adaptable high-throughput screening platform shows great promise for further identification of novel modulators of mitochondrial function, including selective inhibitors of other sites of superoxide/H₂O₂ production. As more potent and selective inhibitors of the numerous sites of superoxide/H₂O₂ production are identified, we can begin to address longstanding questions regarding the role of mitochondrial ROS production in health and disease.

Acknowledgements

Supported by The Ellison Medical Foundation grant AG-SS-2288-09 (MDB) and National Institutes of Health grants R01 AG033542 (MDB), RL1 GM084432 (REH), and TL1 AG032116 (ALO).

Abbreviations

mGPDH	mitochondrial <i>sn</i> -glycerol 3-phosphate dehydrogenase
TPMP	methyltriphenylphosphonium
TMRM	tetramethylrhodamine methyl ester
Ψ_m	potential difference across the mitochondrial inner membrane
pH	pH difference across the mitochondrial inner membrane
site I_F	flavin mononucleotide site of complex I
site I_F/DH	site I _F plus matrix NAD-linked dehydrogenases
site I_Q	ubiquinone-binding site of complex I
site II_F	flavin site of complex II
site III_{Q_o}	outer ubiquinone-binding site of complex III

FCCP	carbonyl cyanide-4-(trifluoromethoxy)phenylhydrazone
CN-POBS	N-cyclohexyl-4-(4-nitrophenoxy)benzenesulfonamide
DMSO	dimethylsulfoxide
ROS	reactive oxygen species.

References

1. Harman D. The free radical theory of aging: Effect of age on serum copper levels. *J. Gerontol.* 1965; 20:151–153. [PubMed: 14284786]
2. Finkel T, Holbrook NJ. Oxidants, oxidative stress and the biology of ageing. *Nature.* 2000; 408:239–247. [PubMed: 11089981]
3. Lin MT, Beal MF. Mitochondrial dysfunction and oxidative stress in neurodegenerative diseases. *Nature.* 2006; 443:787–795. [PubMed: 17051205]
4. Van Gaal LF, Mertens IL, De Block CE. Mechanisms linking obesity with cardiovascular disease. *Nature.* 2006; 444:875–880. [PubMed: 17167476]
5. Muller FL, Lustgarten MS, Jang Y, Richardson A, Van Remmen H. Trends in oxidative aging theories. *Free Rad. Biol. Med.* 2007; 43:477–503. [PubMed: 17640558]
6. Nunnari J, Suomalainen A. Mitochondria: In sickness and in health. *Cell.* 2012; 148:1145–1159. [PubMed: 22424226]
7. Brand MD, Orr AL, Perevoshchikova IV, Quinlan CL. The role of mitochondrial function and cellular bioenergetics in ageing and disease. *Br. J. Dermatol.* 2013; 169(Suppl 2):1–8. [PubMed: 23786614]
8. Brand MD. The sites and topology of mitochondrial superoxide production. *Exp. Gerontol.* 2010; 45:466–472. [PubMed: 20064600]
9. Treberg JR, Quinlan CL, Brand MD. Evidence for two sites of superoxide production by mitochondrial NADH-ubiquinone oxidoreductase (complex I). *J. Biol. Chem.* 2011; 286:27103–27110. [PubMed: 21659507]
10. Betarbet R, Sherer TB, MacKenzie G, Garcia-Osuna M, Panov AV, Greenamyre JT. Chronic systemic pesticide exposure reproduces features of Parkinson's disease. *Nat. Neurosci.* 2000; 3:1301–1306. [PubMed: 11100151]
11. Langston JW, Ballard P, Tetrud JW, Irwin I. Chronic Parkinsonism in humans due to a product of meperidine-analog synthesis. *Science.* 1983; 219:979–980. [PubMed: 6823561]
12. Lambert AJ, Boysen HM, Buckingham JA, Yang T, Podlutzky A, Austad SN, Kunz TH, Buffenstein R, Brand MD. Low rates of hydrogen peroxide production by isolated heart mitochondria associate with long maximum lifespan in vertebrate homeotherms. *Aging Cell.* 2007; 6:607–618. [PubMed: 17596208]
13. Lambert AJ, Buckingham JA, Boysen HM, Brand MD. Low complex I content explains the low hydrogen peroxide production rate of heart mitochondria from the long-lived pigeon, *Columba livia*. *Aging Cell.* 2010; 9:78–91. [PubMed: 19968628]
14. Perevoshchikova IV, Quinlan CL, Orr AL, Gerencser AA, Brand MD. Sites of superoxide and hydrogen peroxide production during fatty acid oxidation in rat skeletal muscle mitochondria. *Free Rad. Biol. Med.* 2013; 61:298–309. [PubMed: 23583329]
15. Quinlan CL, Treberg JR, Perevoshchikova IV, Orr AL, Brand MD. Native rates of superoxide production from multiple sites in isolated mitochondria measured using endogenous reporters. *Free Rad. Biol. Med.* 2012; 53:1807–1817. [PubMed: 22940066]
16. Quinlan CL, Perevoshchikova IV, Hey-Mogensen M, Orr AL, Brand MD. Sites of reactive oxygen species generation by mitochondria oxidizing different substrates. *Redox Biol.* 2013; 1:304–312. [PubMed: 24024165]

17. St-Pierre J, Buckingham JA, Roebuck SJ, Brand MD. Topology of superoxide production from different sites in the mitochondrial electron transport chain. *J. Biol. Chem.* 2002; 277:44784–44790. [PubMed: 12237311]
18. Orr AL, Quinlan CL, Perevoshchikova IV, Brand MD. A refined analysis of superoxide production by mitochondrial *sn*-glycerol 3-phosphate dehydrogenase. *J. Biol. Chem.* 2012; 287:42921–42935. [PubMed: 23124204]
19. Bell EL, Klimova TA, Eisenbart J, Moraes CT, Murphy MP, Budinger GRS, Chandel NS. The Qo site of the mitochondrial complex III is required for the transduction of hypoxic signaling *via* reactive oxygen species production. *J. Cell Biol.* 2007; 177:1029–1036. [PubMed: 17562787]
20. Tormos KV, Anso E, Hamanaka RB, Eisenbart J, Joseph J, Kalyanaraman B, Chandel NS. Mitochondrial complex III ROS regulate adipocyte differentiation. *Cell Metab.* 2011; 14:537–544. [PubMed: 21982713]
21. Weinberg F, Hamanaka R, Wheaton WW, Weinberg S, Joseph J, Lopez M, Kalyanaraman B, Mutlu GM, Budinger GRS, Chandel NS. Mitochondrial metabolism and ROS generation are essential for Kras-mediated tumorigenicity. *Proc. Nat. Acad. Sci.* 2010; 107:8788–8793. [PubMed: 20421486]
22. Hoffman DL, Salter JD, Brookes PS. Response of mitochondrial reactive oxygen species generation to steady-state oxygen tension: Implications for hypoxic cell signaling. *Am. J. Physiol. – Heart Circ. Physiol.* 2007; 292:H101–H108.
23. Kerr DS. Treatment of mitochondrial electron transport chain disorders: A review of clinical trials over the past decade. *Mol. Genet. Metab.* 2010; 99:246–255. [PubMed: 20060349]
24. Gane EJ, Weilert F, Orr DW, Keogh GF, Gibson M, Lockhart MM, Frampton CM, Taylor KM, Smith RAJ, Murphy MP. The mitochondria-targeted anti-oxidant mitoquinone decreases liver damage in a phase II study of hepatitis C patients. *Liver Int.* 2010; 30:1019–1026. [PubMed: 20492507]
25. Snow BJ, Rolfe FL, Lockhart MM, Frampton CM, O'Sullivan JD, Fung V, Smith RAJ, Murphy MP, Taylor KM. A double-blind, placebo-controlled study to assess the mitochondria-targeted antioxidant mitoQ as a disease-modifying therapy in Parkinson's disease. *Mov. Disord.* 2010; 25:1670–1674. [PubMed: 20568096]
26. Affourtit C, Quinlan CL, Brand MD. Measurement of proton leak and electron leak in isolated mitochondria. *Methods Mol. Biol.* 2012; 810:165–182. [PubMed: 22057567]
27. Orr AL, Ashok D, Sarantos MR, Ng R, Shi T, Gerencser AA, Hughes RE, Brand MD. Novel inhibitors of mitochondrial *sn*-glycerol 3-phosphate dehydrogenase. Manuscript in submission.
28. Brideau C, Gunter B, Pikounis B, Liaw A. Improved statistical methods for hit selection in high-throughput screening. *J. Biomol. Screen.* 2003; 8:634–647. [PubMed: 14711389]
29. Malo N, Hanley JA, Cerquozzi S, Pelletier J, Nadon R. Statistical practice in highthroughput screening data analysis. *Nat. Biotech.* 2006; 24:167–175.
30. Lambert AJ, Buckingham JA, Boysen HM, Brand MD. Diphenyleneiodonium acutely inhibits reactive oxygen species production by mitochondrial complex I during reverse, but not forward electron transport. *Biochim. Biophys. Acta.* 2008; 1777:397–403. [PubMed: 18395512]
31. Rogers GW, Brand MD, Petrosyan S, Ashok D, Elorza AA, Ferrick DA, Murphy AN. High throughput microplate respiratory measurements using minimal quantities of isolated mitochondria. *PLoS One.* 2011; 6:e21746. [PubMed: 21799747]
32. Zhang JH, Chung TDY, Oldenburg KR. A simple statistical parameter for use in evaluation and validation of high throughput screening assays. *J. Biomol. Screen.* 1999; 4:67–73. [PubMed: 10838414]
33. Quinlan CL, Gerencser AA, Treberg JR, Brand MD. The mechanism of superoxide production by the antimycin-inhibited mitochondrial Q-cycle. *J. Biol. Chem.* 2011; 286:31361–31372. [PubMed: 21708945]
34. Scaduto RC, Grotyohann LW. Measurement of mitochondrial membrane potential using fluorescent rhodamine derivatives. *Biophys. J.* 1999; 76:469–477. [PubMed: 9876159]
35. Treberg JR, Brand MD. A model of the proton translocation mechanism of complex I. *J. Biol. Chem.* 2011; 286:17579–17584. [PubMed: 21454533]

36. Pryde KR, Hirst J. Superoxide is produced by the reduced flavin in mitochondrial complex I: a single, unified mechanism that applies during both forward and reverse electron transfer. *J. Biol. Chem.* 2011; 286:18056–18065. [PubMed: 21393237]
37. Muller FL, Liu Y, Abdul-Ghani MA, Lustgarten MS, Bhattacharya A, Jang YC, Van Remmen H. High rates of superoxide production in skeletal-muscle mitochondria respiring on both complex I- and complex II-linked substrates. *Biochem. J.* 2008; 409:491–499. [PubMed: 17916065]
38. Kaminski MM, Sauer SW, Kaminski M, Opp S, Ruppert T, Grigaravicius P, Grudnik P, Gröne HJ, Krammer PH, Gülow K. T cell activation is driven by an ADP-dependent glucokinase linking enhanced glycolysis with mitochondrial reactive oxygen species generation. *Cell Rep.* 2012; 2:1300–1315. [PubMed: 23168256]
39. Folbergrova J, Ljunggren B, Norberg K, Siesjö BK. Influence of complete ischemia on glycolytic metabolites, citric acid cycle intermediates, and associated amino acids in the rat cerebral cortex. *Brain Res.* 1974; 80:265–279. [PubMed: 4154061]
40. Benzi G, Arrigoni E, Marzatico F, Villa RF. Influence of some biological pyrimidines on the succinate cycle during and after cerebral ischemia. *Biochem. Pharm.* 1979; 28:2545–2550. [PubMed: 518665]
41. Sanderson T, Reynolds C, Kumar R, Przyklenk K, Hüttemann M. Molecular mechanisms of ischemia–reperfusion injury in brain: Pivotal role of the mitochondrial membrane potential in reactive oxygen species generation. *Mol. Neurobiol.* 2013; 47:9–23. [PubMed: 23011809]
42. Chouchani ET, Methner C, Nadtochiy SM, Logan A, Pell VR, Ding S, James AM, Cocheme HM, Reinhold J, Lilley KS, Partridge L, Fearnley IM, Robinson AJ, Hartley RC, Smith RAJ, Krieg T, Brookes PS, Murphy MP. Cardioprotection by S-nitrosation of a cysteine switch on mitochondrial complex I. *Nat. Med.* 2013; 19:753–759. [PubMed: 23708290]
43. Niatetskaya ZV, Sosunov SA, Matsiukevich D, Utkina-Sosunova IV, Ratner VI, Starkov AA, Ten VS. The oxygen free radicals originating from mitochondrial complex I contribute to oxidative brain injury following hypoxia–ischemia in neonatal mice. *J. Neurosci.* 2012; 32:3235–3244. [PubMed: 22378894]

succinate reduce the mobile ubiquinone pool (Q-pool) before ultimately reducing O_2 at complex IV (solid line with arrowheads). Electron transfer through complex III and complex IV drives the pumping of protons to the intermembrane space resulting in an electrochemical gradient of protons across the inner membrane (proton motive force, PMF, composed of a pH gradient, ΔpH , and a membrane potential, $\Delta \Psi$). The combination of a reduced Q-pool and high PMF drives the reverse transport of electrons from the Q-pool to NAD^+ in the matrix *via* complex I (dashed line with arrowheads). Under this condition, most of the $O_2^{\bullet-}/H_2O_2$ production is from site I_Q although a minor portion comes from site I_F/DH and site III_{Q_0} [16]. Site II_F $O_2^{\bullet-}/H_2O_2$ production is inhibited by high succinate and mGPDH is substrate-limited. The protonophore FCCP dissipates PMF causing an oxidation of all redox centers and acts as a positive control for this assay. An alternative assay utilizing subsaturating succinate was also used during compound retesting. In this condition, site I_Q remains active but contributes proportionally less $O_2^{\bullet-}/H_2O_2$ due to lower PMF and increased activity from site II_F . **(B)** Site I_F/DH with 5 mM malate, 5 mM glutamate and 4 μM rotenone. Malate is oxidized to oxaloacetate by malate dehydrogenase (MDH) to generate NADH that is oxidized by site I_F . Glutamate is added to convert oxaloacetate to 2-oxoglutarate and aspartate by aspartate aminotransferase (AAT) and facilitate the continual uptake and oxidation of malate. Rotenone prevents oxidation of redox centers upstream of site I_Q . This increases the matrix NADH/ NAD^+ ratio to induce $O_2^{\bullet-}$ production from site I_F while oxidizing redox centers downstream of complex I. The formation of 2-oxoglutarate in the presence of a high NADH/ NAD^+ ratio also induces significant $O_2^{\bullet-}/H_2O_2$ production from 2-oxoglutarate dehydrogenase (OGDH). The addition of 20 mM aspartate disfavors the transamination of oxaloacetate to 2-oxoglutarate resulting in lower $O_2^{\bullet-}/H_2O_2$ production from both site I_F and OGDH and is used as a positive control for this assay. **(C)** Site II_F with 15 μM palmitoylcarnitine, 2 μM myxothiazol and 2.5 μM antimycin A. After reaction with coenzyme A, palmitoylcarnitine is metabolized by enzymes of the β -oxidation pathway to yield acetyl-CoA and NADH as well as reducing equivalents that enter the Q-pool *via* electron transferring flavoprotein (ETF) and ETF:ubiquinone oxidoreductase (ETFQR). Oxidation of the Q-pool is prevented by myxothiazol and antimycin A, facilitating the backward entry of electrons into complex II and the production of $O_2^{\bullet-}/H_2O_2$ from site II_F (dashed line with arrowheads). Site II_F predominates heavily in this condition, although low levels of production from site I_F/DH are also observed due to the NADH generated during β -oxidation and TCA cycle activity. Malonate potently inhibits this production from site II_F and is used as a positive control in this assay. **(D)** Site III_{Q_0} with 5 mM succinate, 4 μM rotenone and 2.5 μM antimycin A. In the presence of rotenone and antimycin A, the oxidation of succinate strongly reduces the Q-pool. Blockade of site III_{Q_i} by antimycin A promotes $O_2^{\bullet-}$ production from site III_{Q_0} to both sides of the inner membrane. The saturating levels of succinate prevent $O_2^{\bullet-}/H_2O_2$ production from site II_F while rotenone and a lack of PMF prevent production from site I_Q . Site I_F/DH has a minor contribution due to a small increase in matrix NADH due to Krebs cycle activity. Myxothiazol potently inhibits site III_{Q_0} and is used as a positive control in this assay. An alternative assay utilizing subsaturating succinate was also used during compound retesting. In this condition, partial reduction of the Q-pool results in maximal $O_2^{\bullet-}/H_2O_2$ production from site III_{Q_0} . However, unlike with saturating succinate, putative inhibitors may cause a lower signal simply through partial inhibition of succinate oxidation. **(E)** mGPDH with 25 mM glycerol phosphate, 4 μM

rotenone, 2.5 μM antimycin A, 1 mM malonate and 2 μM myxothiazol. Oxidation of glycerol 3-phosphate causes an over-reduction of redox centers in mGPDH when the oxidation of the Qpool is prevented by myxothiazol and antimycin A. This results in $\text{O}_2^{\bullet-}/\text{H}_2\text{O}_2$ production from mGPDH towards both sides of the inner membrane. $\text{O}_2^{\bullet-}/\text{H}_2\text{O}_2$ production is prevented at site I_Q , site II_F and site III_{Q_0} by rotenone, malonate and myxothiazol, respectively. Site $\text{I}_\text{F}/\text{DH}$ is fully oxidized under this condition. There were no positive controls used for this assay; instead, signals were scaled to the signals with FCCP in the site I_Q assay. (F) Ψ_m with 5 mM malate, 5 mM glutamate and 80 $\text{ng} \cdot \text{mL}^{-1}$ nigericin. Malate and glutamate are metabolized as described in the site $\text{I}_\text{F}/\text{DH}$ assay. However, in the absence of rotenone, electrons are transported to reduce O_2 at complex IV with proton pumping by complexes I, III and IV generating a PMF. The pH component of PMF is converted to Ψ_m by the addition of the K^+/H^+ exchanger nigericin. The uptake of the fluorescent cation TMRM into the mitochondrial matrix reports Ψ_m . The protonophore FCCP dissipates PMF and acts as a positive control for this assay. $\text{O}_2^{\bullet-}$, superoxide; PMF, proton motive force across the mitochondrial inner membrane; Q-pool, mobile ubiquinone pool; MDH, malate dehydrogenase; OGDH, 2-oxoglutarate dehydrogenase; AAT, aspartate aminotransferase; ETF, electron transferring flavoprotein; ETFQOR, ETF:ubiquinone oxidoreductase; $\text{G}_{\text{F}/\text{Q}}$, FAD and ubiquinone-binding sites in mGPDH.

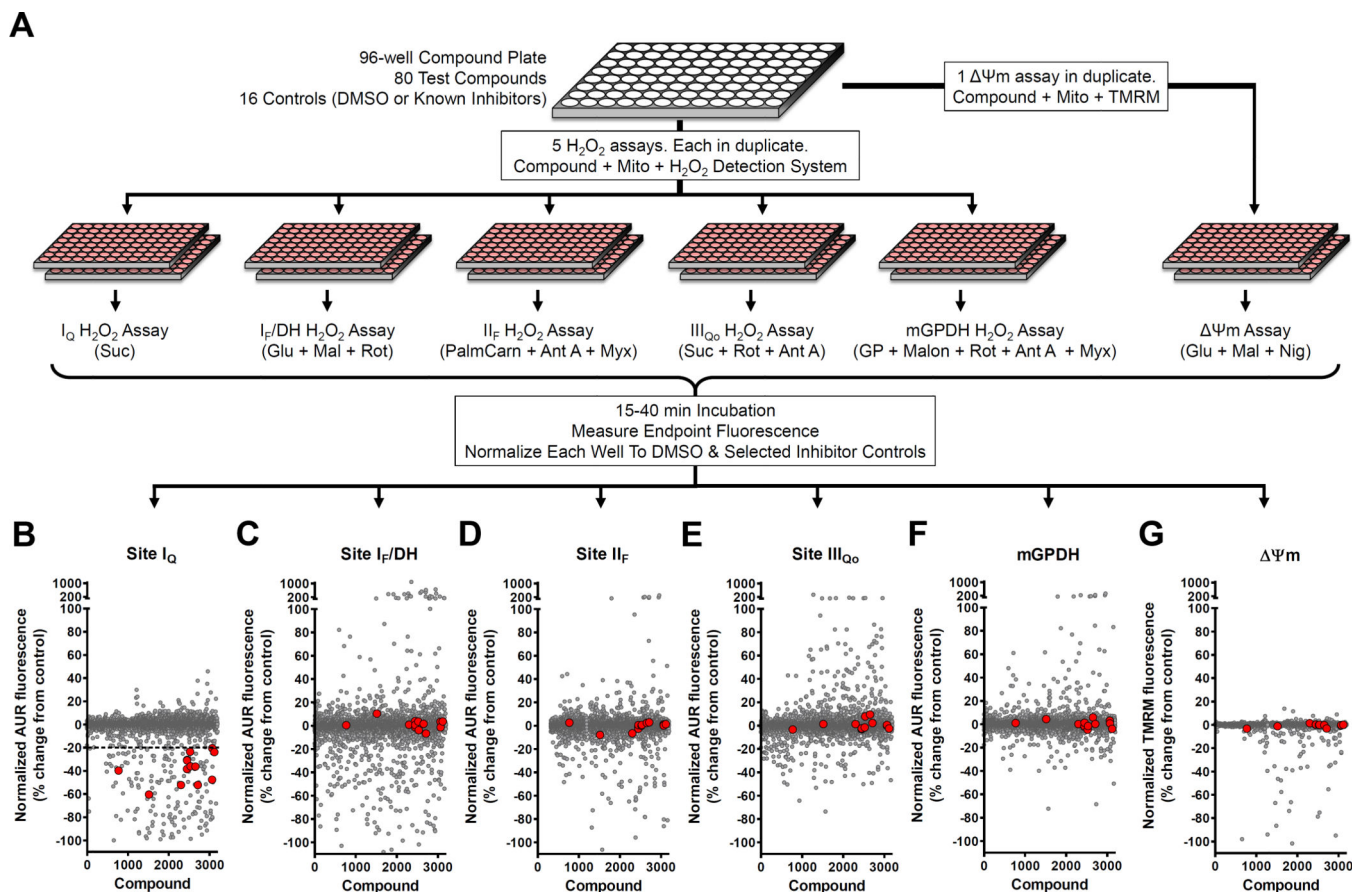


Figure 2. Multiple-parallel screening identifies site-specific inhibitors of H_2O_2 production that do not impair mitochondrial function

(A) Screening workflow. Compounds in 96-well plates were screened in duplicate against the six assays in Fig. 1. Five assays each targeted a distinct site of superoxide/ H_2O_2 production using different substrates without or with inhibitors. The sites assayed were site I_Q , site I_F/DH , site II_F , site III_{Qo} , and mGPDH. A sixth parallel assay of Ψ_m counterscreened for general inhibitors of mitochondrial function. All assays were initiated by the addition of Start Solutions containing the substrates and inhibitors listed in parentheses. Details are in "Experimental procedures" and Fig. 1. Endpoint fluorescence was measured and the effect of compounds was scaled to positive and negative controls included on each assay plate. (B – G) Average normalized effects of 3200 compounds screened against all six assays in duplicate (gray circles). 180 compounds gave >20% inhibition of site I_Q superoxide/ H_2O_2 production (dashed line in B). However, after evaluating their effects in the other screens, only 13 were selective for superoxide/ H_2O_2 production at site I_Q and did not alter Ψ_m (red circles in B – G). AUR, resorufin product of Amplex UltraRed oxidation; Suc, succinate; Glu, glutamate; Mal, malate; PalmCarn, palmitoylcarnitine; GP, glycerol 3-phosphate; Rot, rotenone; Ant A, antimycin A; Myx, myxothiazol; Malon, malonate; Nig, nigericin.

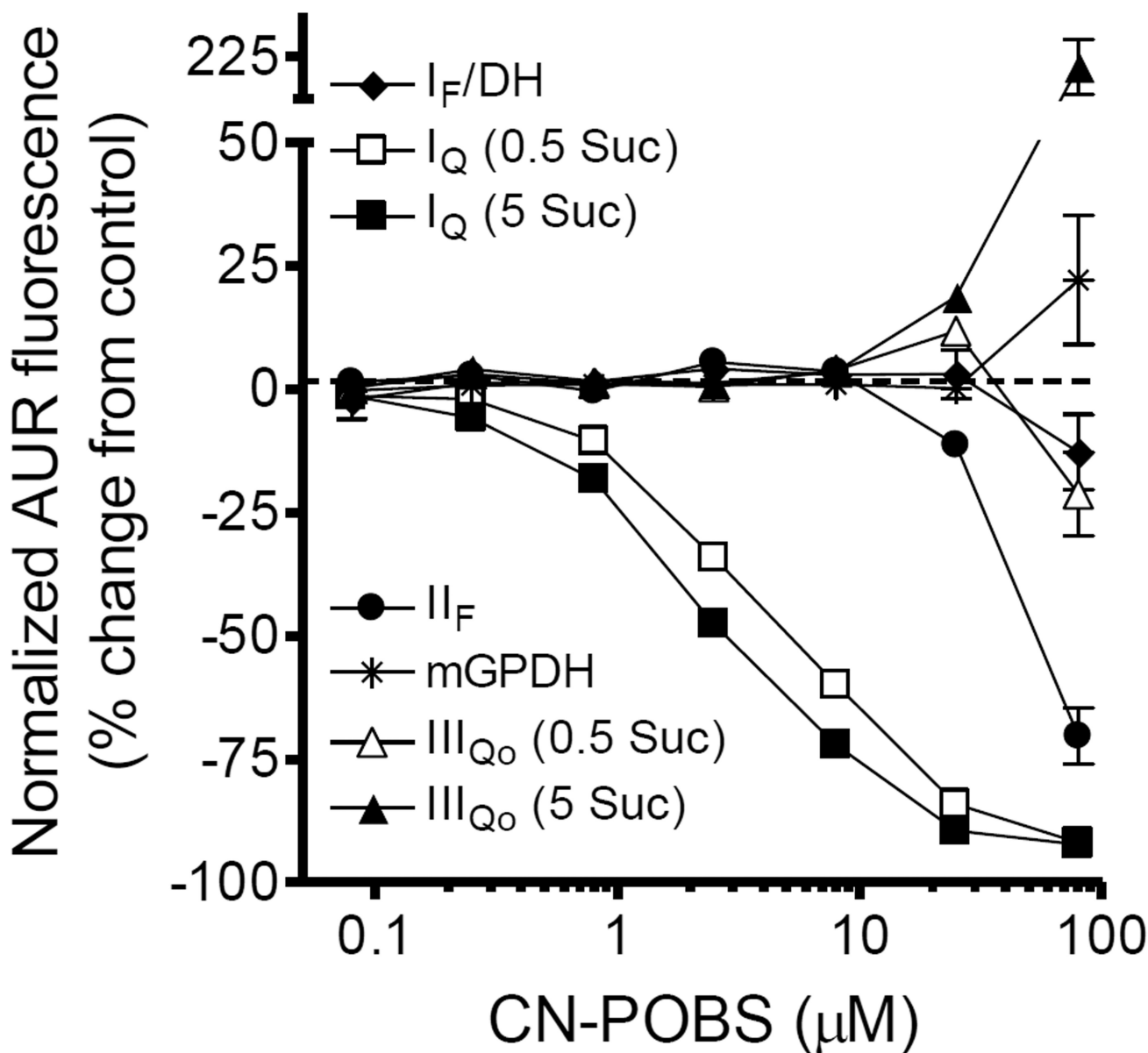


Figure 3. CN-POBS is a selective inhibitor of superoxide/H₂O₂ production from site I_Q
 Effect of CN-POBS on normalized H₂O₂ production from site I_F/DH (black diamonds), site I_Q (with 0.5 or 5 mM succinate; white and black squares, respectively), site II_F (black circles), mGPDH (black stars), and site III_{Qo} (with 0.5 or 5 mM succinate; white and black triangles, respectively). Details of the conditions to induce H₂O₂ production from each site are given in "Experimental procedures" and Fig. 1. Data are normalized means ± S.E. (n = 3). AUR, resorufin product of Amplex UltraRed oxidation; Suc, succinate.

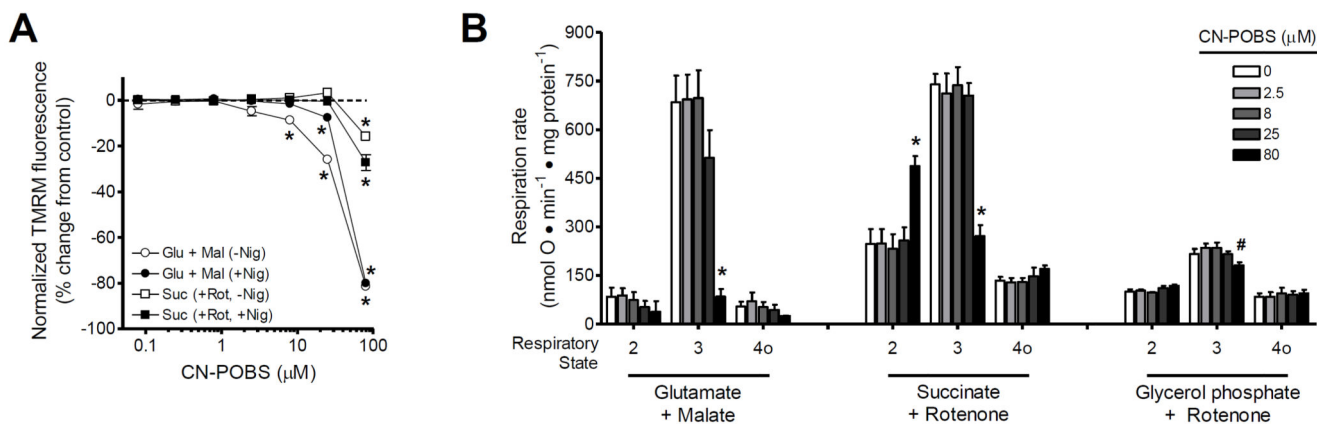


Figure 4. CN-POBS does not inhibit Ψ_m or respiration below 8 μM

(A) Effect of CN-POBS on normalized Ψ_m generated by oxidation of 5 mM glutamate plus 5 mM malate without or with 80 $\text{ng} \cdot \text{mL}^{-1}$ nigericin (white or black circles), or 5 mM succinate and 4 μM rotenone without or with nigericin (white or black triangles). Ψ_m with glutamate plus malate in the absence of nigericin was significantly decreased by 8, 25 and 80 μM CN-POBS and in the presence of nigericin only by 25 and 80 μM CN-POBS. Ψ_m with succinate was significantly decreased by 80 μM CN-POBS. (* $p < 0.05$ versus vehicle control; one-way ANOVA with Newman-Keuls post-test). Data are normalized means \pm S.E. (n = 3). Glu, glutamate; Mal, malate; Nig, nigericin; Suc, succinate; Rot, rotenone. (B) Effect of CN-POBS on the rates of mitochondrial respiration driven by 5 mM glutamate plus 5 mM malate, 5 mM succinate with 4 μM rotenone, or 16.7 mM glycerol phosphate with 4 μM rotenone and 250 nM free calcium. Respiratory states 2, 3, and 4o were defined by the sequential additions of substrate, 5 mM ADP, and 0.5 $\mu\text{g} \cdot \text{mL}^{-1}$ oligomycin, respectively. CN-POBS at 80 μM significantly decreased state 3 respiration with all substrates and increased state 2 respiration with succinate. (* $p < 0.05$ versus vehicle control or # $p < 0.05$ versus 2.5 and 8 μM CN-POBS; one-way ANOVA with Newman-Keuls post-test). Data are means \pm S.E. (n = 3).

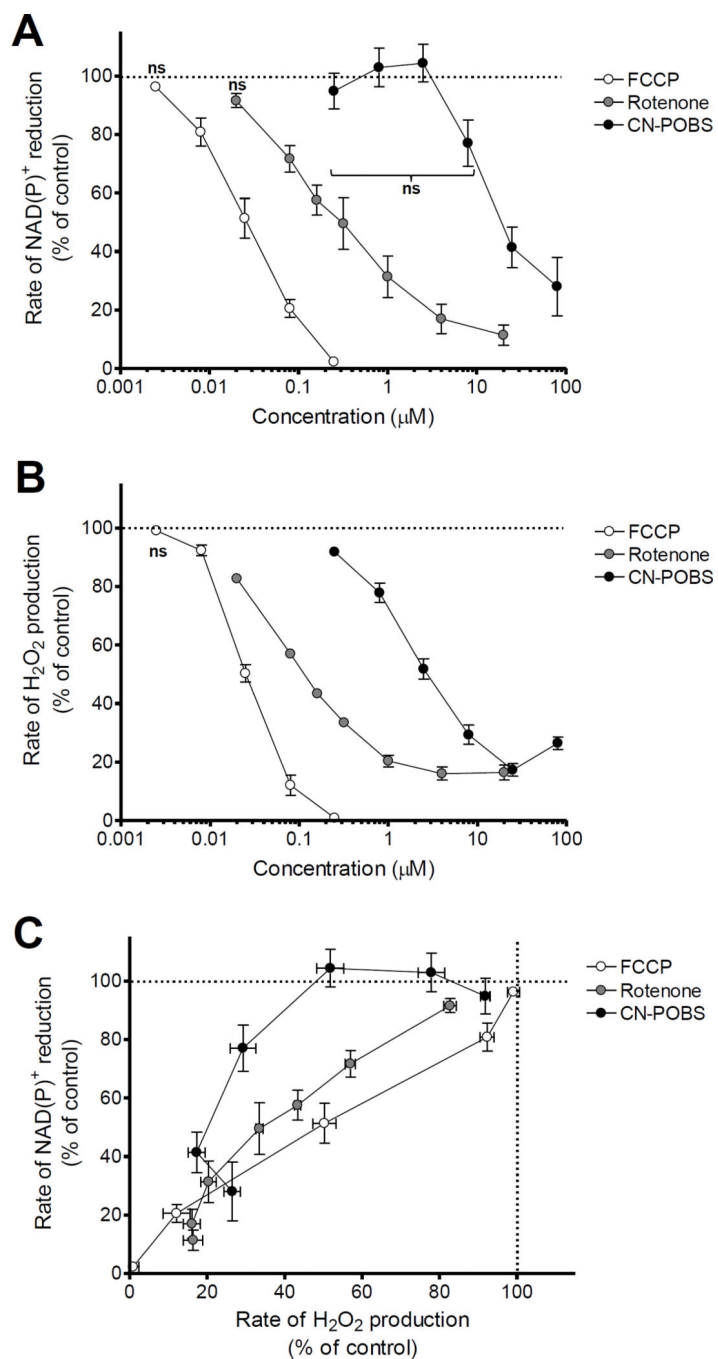


Figure 5. CN-POBS significantly lowers H₂O₂ production at site I_Q without altering electron flux through complex I

(A) Effect of FCCP (white circles), rotenone (gray circles), and CN-POBS (black circles), on normalized rates of NAD(P)⁺ reduction driven by 5 mM succinate plus 0.5 mM glutamate. FCCP significantly lowered the rate of NAD(P)⁺ reduction at all concentrations except 0.0025 μM. Rotenone significantly lowered the rate of NAD(P)⁺ reduction at all concentrations except 0.02 μM. CNPOBS lowered the rate of NAD(P)⁺ reduction at 25 and 80 μM. (ns = not significant. All other points significant at $p < 0.05$; one-way ANOVA with

Newman-Keuls post-test). Data are means \pm S.E. ($n = 3 - 5$). **(B)** Effect of FCCP (white circles), rotenone (gray circles), and CN-POBS (black circles), on normalized rates of H_2O_2 production driven by 5 mM succinate plus 0.5 mM glutamate. All three compounds significantly decreased the rate of H_2O_2 production at all concentrations except FCCP at 0.0025 μ M. (ns = not significant. All other points significant at $p < 0.05$; one-way ANOVA with Newman-Keuls post-test). Data are means \pm S.E. ($n = 4$). **(C)** Replot of the data in A and B to reveal the effect of FCCP (white circles), rotenone (gray circles), and CN-POBS (black circles) on the rates of $NAD(P)^+$ reduction relative to their effects on the normalized rates of H_2O_2 production. CN-POBS was more effective than either FCCP or rotenone at decreasing the rate of H_2O_2 production without inhibiting the rate of $NAD(P)^+$ reduction.

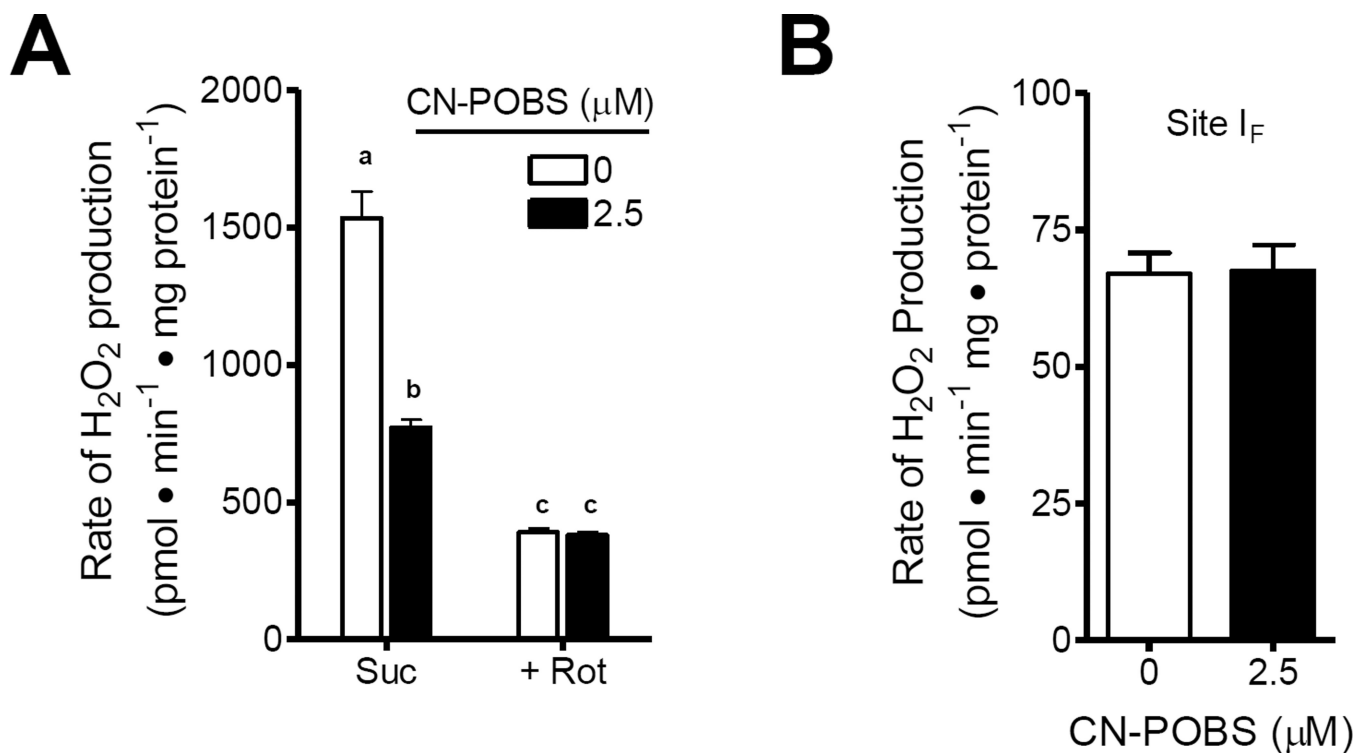


Figure 6. CN-POBS suppresses the majority of the superoxide/H₂O₂ production from site I_Q without inhibiting superoxide/H₂O₂ production from site I_F

(A) Effect of 2.5 μM CN-POBS on the rate of H₂O₂ production driven by 5 mM succinate only (left hand set of columns) or by 5 mM succinate with 4 μM rotenone (right hand set of columns). CN-POBS significantly inhibited 67% of the rotenone-sensitive H₂O₂ production (from site I_Q) driven by succinate alone but had no significant effect on H₂O₂ production by succinate in the presence of rotenone (from site I_F/DH). ($p < 0.01$ between conditions indicated by different letters; two-way ANOVA with Bonferroni post-test). Data are means ± S.E. (n = 3). Suc, succinate; Rot, Rotenone. (B) Effect of 2.5 μM CN-POBS on the rate of H₂O₂ production driven by 5 mM malate in the presence of 2.5 mM ATP, 1.5 mM aspartate, 4 μM rotenone and 1 μg • mL⁻¹ oligomycin. CN-POBS had no effect on H₂O₂ production (specifically from site I_F) in this condition. Data are means ± S.E. (n = 3).

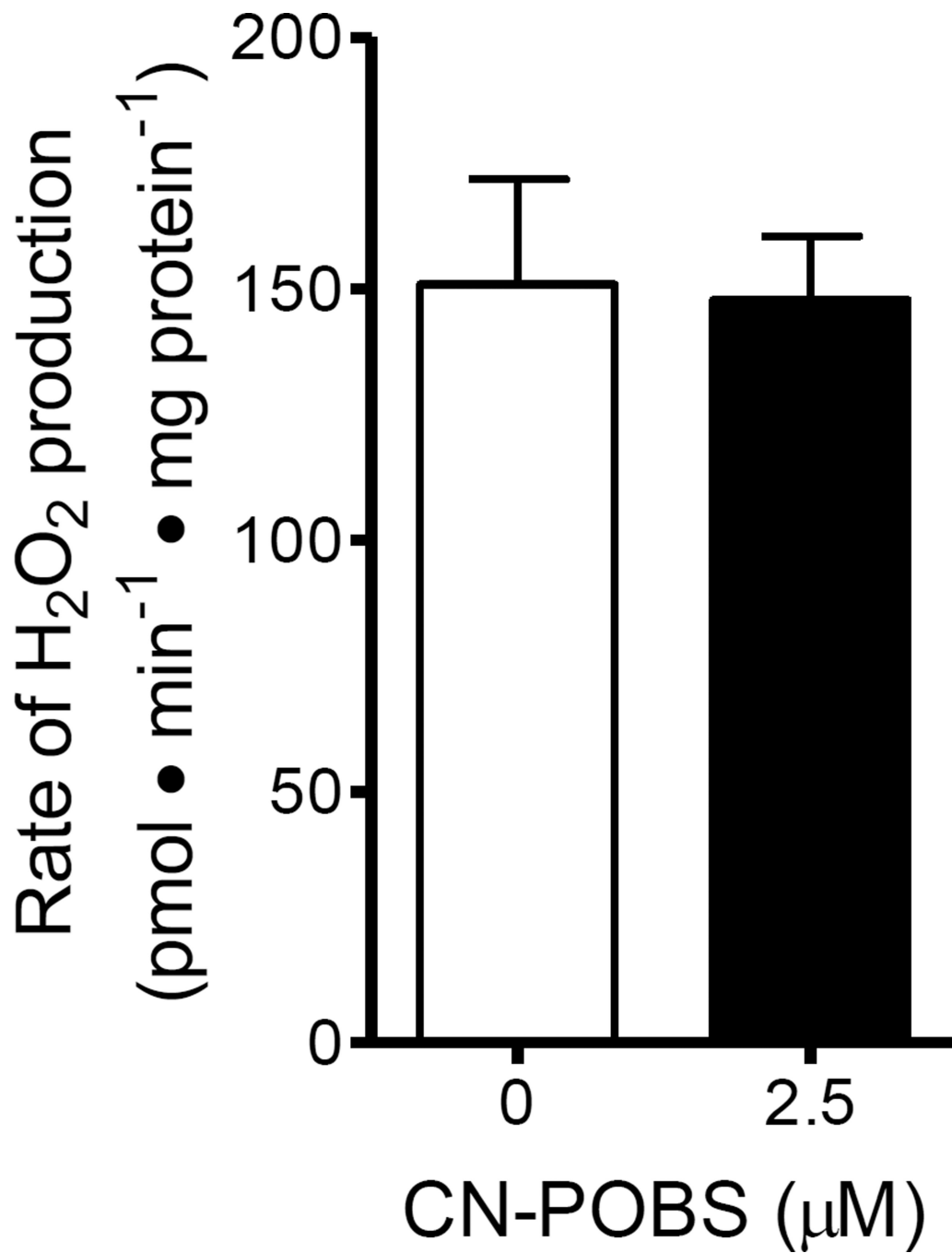


Figure 7. Site I_Q is not active during forward electron transport driven by glutamate plus malate CN-POBS had no effect on the rate of H₂O₂ production driven by 5 mM glutamate plus 5 mM malate under non-phosphorylating conditions. Data are means ± S.E. (n = 4).

Table 1

Summary statistics for the screen

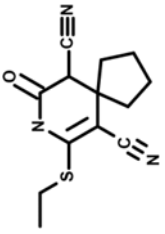
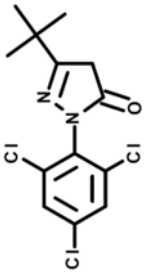
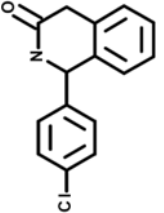
Coefficients of variation (%CV) were determined from eight DMSO control wells included on each assay plate (n = 36 plates). Z-factors [32] were calculated using raw average fluorescence values and their standard deviations for DMSO controls and selected inhibitor controls (Z-factor comparisons shown) included on each assay plate (n = 36 plates). Total Hits are the numbers of compounds that surpassed the threshold set for each individual assay, whereas Selective Hits are the numbers of compounds remaining after excluding those that also surpassed a minimum threshold in at least one of the other five assays (see "Hit Selection" in "Experimental procedures" for threshold cutoffs).

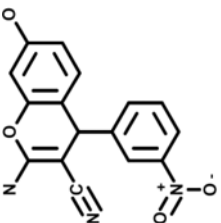
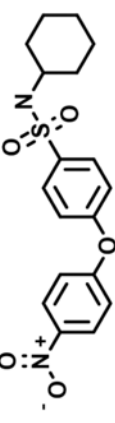
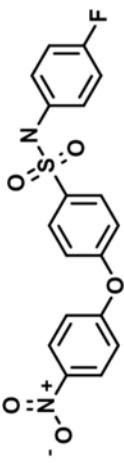
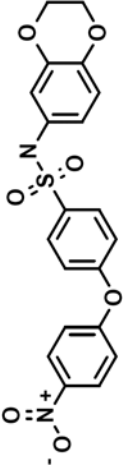
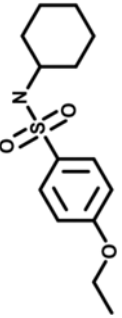
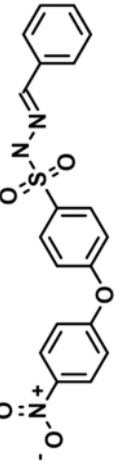
Assay	%CV	Z-Factor	Z-Factor Comparison	Total Hits	Selective Hits
I _Q	3.4 ± 0.3	0.88 ± 0.01	DMSO vs FCCP	180	13
I _F /DH	4.5 ± 0.4	0.62 ± 0.02	DMSO vs Aspartate	199	17
II _F	6.3±0.6	0.54 ± 0.04	DMSO vs Malonate	80	4
III _{Q₀}	4.8 ± 0.4	0.77 ± 0.02	DMSO vs Myxothiazol	72	13
mGFDH	3.4 ± 0.2	n.d.	n.a.	87	8
Ψ _m	2.2 ± 0.4	0.87 ± 0.03	DMSO vs FCCP	n.a.	n.a.

Table 2

Partial list of selective suppressors of superoxide/H₂O₂ production from site I_Q, select structural analogs, and their effects on H₂O₂ production, Ψ_m and the rate of NAD(P)⁺ reduction from succinate *via* complex I

Summary of effects on H₂O₂ production and Ψ_m of five compounds identified in the primary screen and ten structural analogs of one of these (CN-POBS). Dose-response curves between 0.08 and 80 μ M were generated for each compound against the five sites of superoxide/H₂O₂ production (sites I_Q, I_F/DH, II_F, III_{Q₀} and mGPDH) and Ψ_m assayed in the primary screen (data not shown; see Experimental procedures). IC₅₀ values in the site I_Q assay were estimated to determine relative potency against this site and relative selectivity in the other five assays. Estimated IC₅₀ values were defined as the tested concentration, or the average of two tested concentrations (gray boxes), that yielded a normalized decrease of ~50% in site I_Q superoxide/H₂O₂ production. The relative selectivity of inhibitors or analogs against the other assays was then compared at these defined IC₅₀ values (or at 80 μ M for compound **15**). The five most potent and selective compounds were tested further for effects on the rate of NAD(P)⁺ reduction by succinate *via* complex I (rightmost column). LogP values are from the NCBI PubChem compound database. Values for all assays are the average of the normalized percent changes from DMSO for two duplicate runs, n.d., not determined.

Compound	ChemBridge ID	Structure	LogP	IC ₅₀ (μ M)	I _Q	I _F /DH	II _F	III _{Q₀}	mGPDH	Ψ_m	Rate of NAD(P) ⁺ Reduction
1	5212116		2.2	2.5	-52	-7	3	2	0	-3	n.d.
2	5192566		4.6	2.5	-57	5	-10	-6	0	-1	n.d.
3	5619111		3.0	25	-56	-6	-30	-5	-3	-1	n.d.

Compound	ChemBridge ID	Structure	LogP	IC ₅₀ (μ M)	I _Q	I _F /DH	II _F	III _{Q₀}	mGPDH	Ψ m	Rate of NAD(P) ⁺ Reduction
4	5154627		2.8	25	-49	8	-21	3	-5	-2	n.d.
CN-POBS	5229982		4.1	4.5	-56	7	4	0	-2	-1	-1
6	5918711		4.5	0.45	-48	-1	1	1	0	-1	-14
7	6669125		4.8	0.8	-51	0	4	-1	-3	-1	-6
8	6491212		3.0	8	-57	2	-3	1	1	-2	6
9	5315316		3.9	16	-54	-7	-6	0	-2	-1	n.d.

Compound	ChemBridge ID	Structure	LogP	IC ₅₀ (μ M)	I _F /DH	II _F	III _{Q₀}	mGPDH	Ψ m	Rate of NAD(P) ⁺ Reduction
10	5229983		3.6	0.8	1	-10	2	1	0	2
11	5229985		3.3	25	8	-43	-16	-7	0	n.d.
12	5109687		2.5	45	-30	-5	45	4	-5	n.d.
13	9040813		2.8	80	30	-11	38	14	-2	n.d.
14	7954145		4.3	-25	-17	8	89	14	-12	n.d.
15	7965586		2.1	>>80	20	-1	2	2	0	n.d.

Table 3
Effect of CN-POBS on Ψ_m and the reduction levels of NAD(P)H and cytochrome b_{566} in mitochondria oxidizing succinate or glutamate plus malate

Ψ_m and the redox states of NAD(P)H and cytochrome b_{566} were determined under the conditions listed in parallel to measurements of H_2O_2 production in Fig. 6 and Fig. 7. In addition, $80 \text{ ng} \cdot \text{ml}^{-1}$ nigericin was added to measurements of Ψ_m to determine if CN-POBS altered Ψ_m . There were no significant differences between DMSO vehicle and $2.5 \mu\text{M}$ CN-POBS for any measurements, or in % reduced NAD(P)H with 5 mM succinate versus succinate plus $4 \mu\text{M}$ rotenone for either DMSO vehicle or CN-POBS. Data are means \pm S.E. (n = 3). The reduction state of cytochrome b_{566} in mitochondria oxidizing succinate in the presence of rotenone was $58.8 \pm 1.2\%$ (mean \pm SE, n = 14) and was not significantly different from that observed with succinate alone ($p = 0.18$, Student's *t*-test). This measurement was not performed in parallel with the others and therefore was not included in the table.

Condition	Ψ_m (mV)		% reduced NAD(P)H		% reduced cytochrome b_{566}	
	0	2.5	0	2.5	0	2.5
Succinate	147.0 ± 3.1	150.8 ± 2.3	86.0 ± 3.1	85.8 ± 2.5	55.0 ± 0.6	57.1 ± 0.5
Succinate + Nigericin	186.0 ± 4.8	186.9 ± 3.3				
Succinate + Rotenone			75.7 ± 3.3	77.0 ± 3.7		
Glutamate + Malate + Oligomycin	143.8 ± 4.7	144.8 ± 0.7	91.7 ± 0.6	92.5 ± 0.8	41.7 ± 1.6	39.8 ± 2.1
Glutamate + Malate + Oligomycin + Nigericin	166.2 ± 3.6	164.8 ± 0.6				